Modeling the Mulit-peak Structure of Solar Cycle

Youwei Yan

Simon Fraser University

August 1, 2022

Solar Cycle

- Driven by the magnetic field of the Sun, solar activity follows an 11-year cyclic pattern, known as the solar cycle.
- The solar cycle can be observed through proxy variables, including the sunspot numbers (SSNs), sunspot areas and 10.7cm flux.

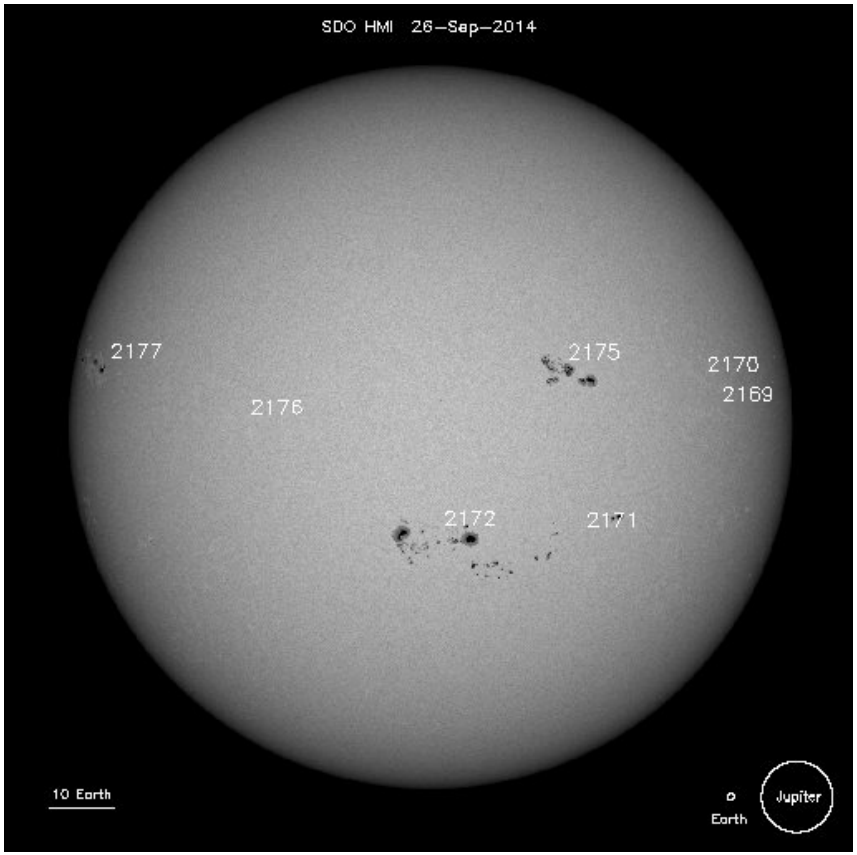

Sunspots observed on Sun's photosphere. (Image courtesy of NASA/SDO)

Solar Cycle

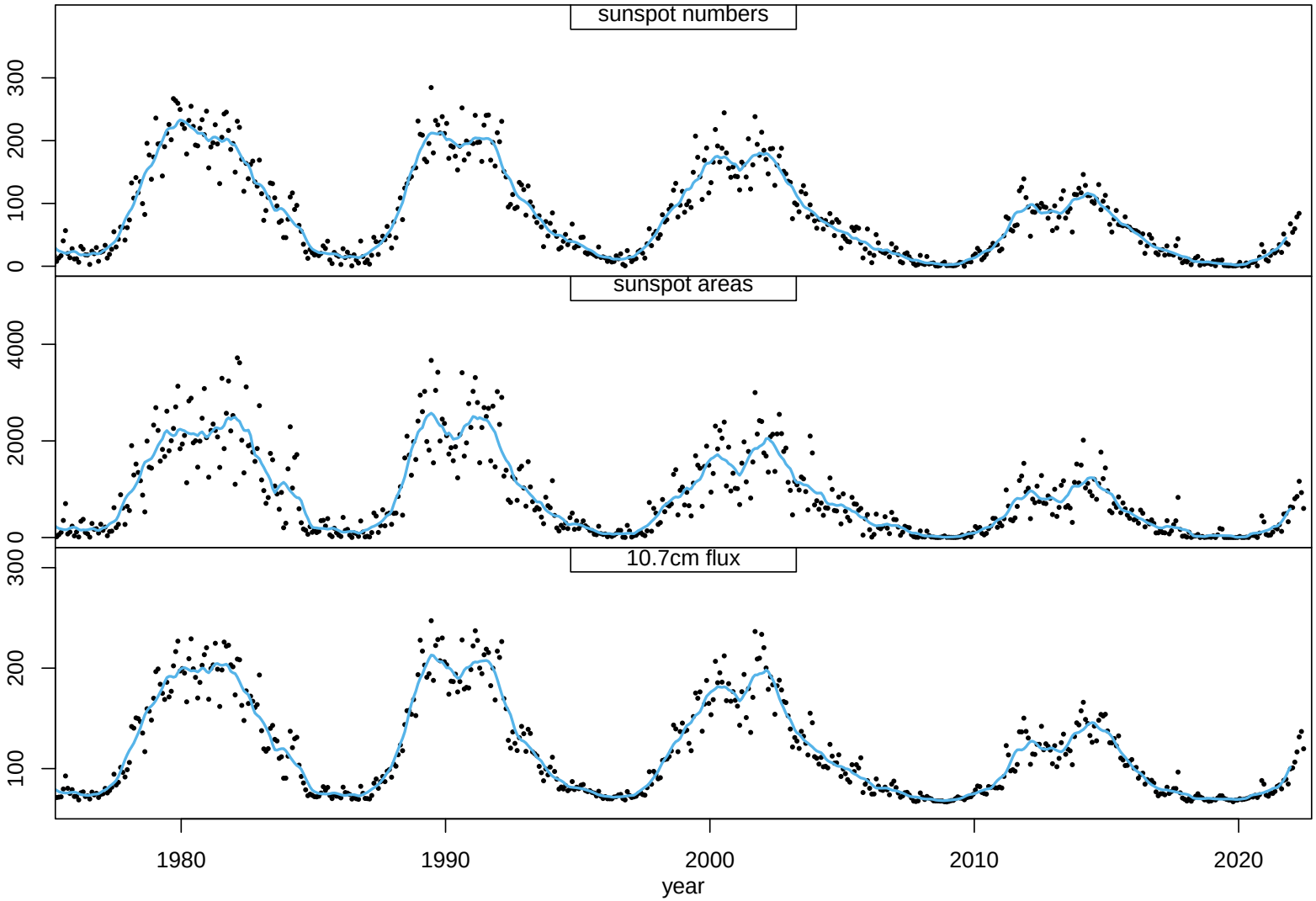
sunspot numbers
0
100
200
300
sunspot areas
0
2000
4000
10.7cm flux
100
200
300
1980
1990
2000
2010
2020
year

Solar Cycle

- Multi-peak structure has been observed in past cycles.
- Our goal is to model the solar cycle and accommodate its potential multi-peak structure.

The Yu et al. (2012) Model

- A Bayesian two-level model that fits the monthly mean SSNs.
- The first level parameterizes the shape of a sunspot cycle into a rising phase and a declining phase.
- The second level describes the evolution of the solar cycle through a set of correlations between the cycle parameters.
- A good model to build upon given its great predictive performance.

The First Level

- The rising phase:

$$U_t = c^{(i)} \left[1 - \left(\frac{t_{\max}^{(i)} - t}{t_{\max}^{(i)} - t_0^{(i)}} \right)^{\alpha_1} \right]$$

for $t < t_{\max}^{(i)}$

- The declining phase:

$$U_t = c^{(i)} \left[1 - \left(\frac{t - t_{\max}^{(i)}}{t_1^{(i)} - t_{\max}^{(i)}} \right)^{\alpha_2} \right]$$

for $t > t_{\max}^{(i)}$

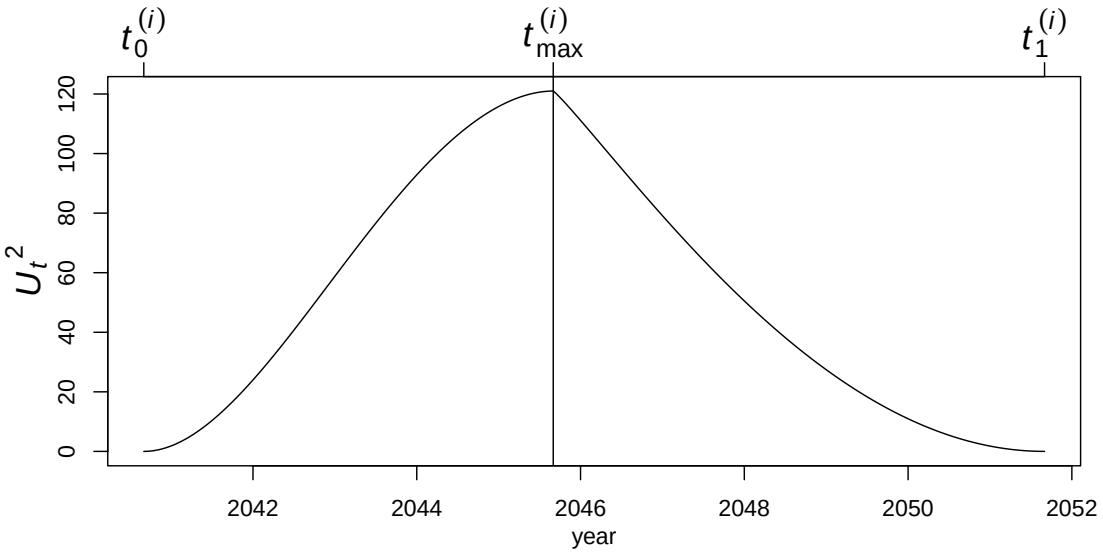

- For cycle i, $c^{(i)}$ is the cycle amplitude, $t_0^{(i)}$ is the start time, $t_{\max}^{(i)}$ is the time of cycle maximum, $t_1^{(i)}$ is the end time, and U_t is "average solar activity level" at time t.

The Second Level

- A set of sequential correlations between the cycle parameters that can be used to predict the parameter values for the following cycle.

$$\begin{aligned}
\text{cycle amplitude,} \quad & c^{(i+1)} \sim \delta_1 + \gamma_1 \frac{c^{(i)}}{t_0^{(i+1)} - t_{\max}^{(i)}} + N(0, \tau_1^2) \\
\text{rise time,} \quad & t_{\max}^{(i+1)} - t_0^{(i+1)} \sim \delta_2 + \gamma_2 c^{(i+1)} + N(0, \tau_2^2) \\
\text{fall time,} \quad & t_1^{(i+1)} - t_{\max}^{(i+1)} \sim \delta_3 + \gamma_3 c^{(i+1)} + N(0, \tau_3^2) \\
\text{start time,} \quad & t_0^{(i+1)} \sim t_1^{(i)} + N(0, \tau_0^2)
\end{aligned}$$

Predictions based on Yu et al. Model

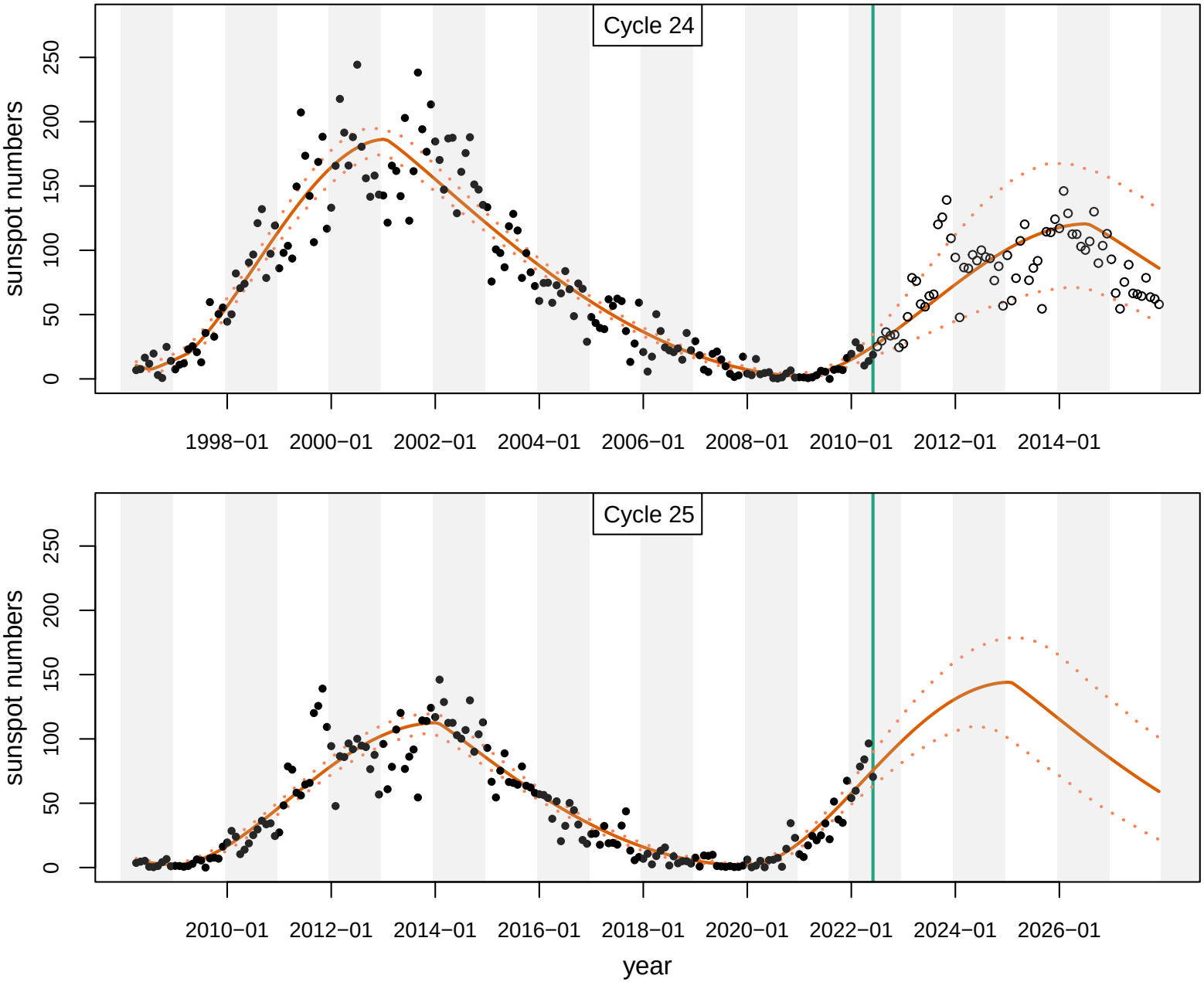

Modeling the Multi-peak Structure

- The Yu et al. model has good predictive performance but it is limited by its single-peak assumption.
- We decide to model the discrepancy between the model expected SSNs and the observed SSNs using Gaussian Process Regression.

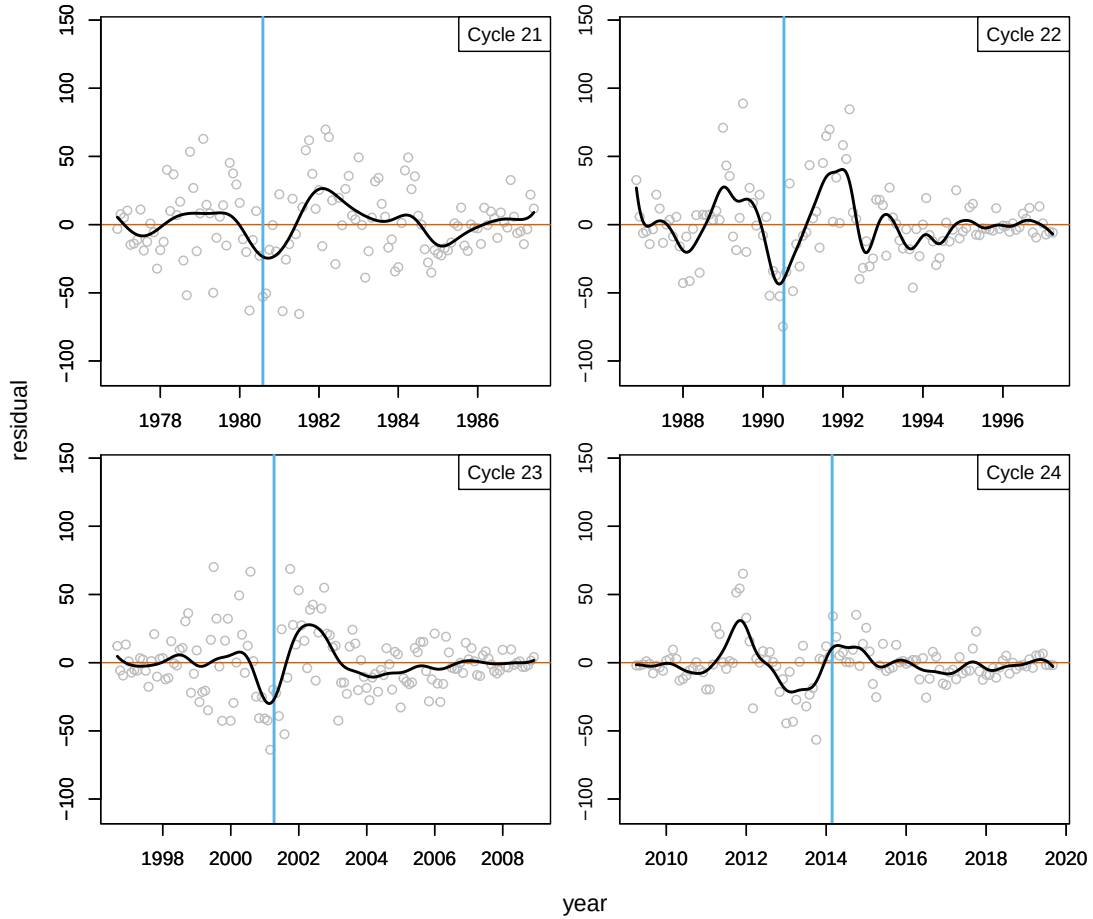

Polar Flux

- The magnitude of the polar flux at cycle minimum is positively correlated with the peak strength of the following sunspot cycle. This correlation has been explained by the dynamo theory.
- Polar flux data, shifted by 5 yrs 1 mo (empirically chosen to maximize correlation with the SSNs), are incorporated into the GP model as inputs.

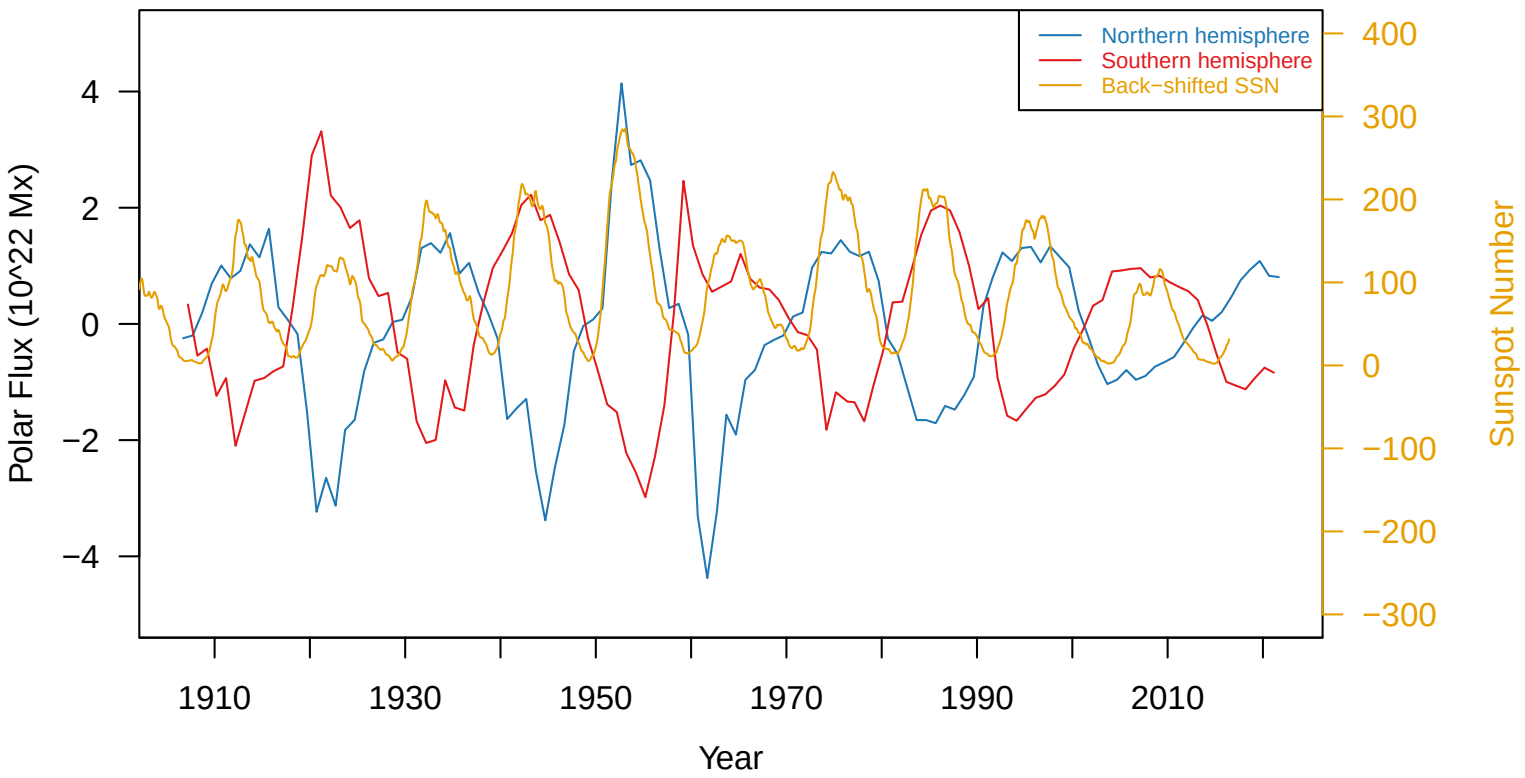

Input Variables for GP

- **Time in cycle**: 0 represents the start of a cycle, 0.5 represents the peak time and 1 represents the end. Posterior means from the Yu et al. are used.
- **Scaled polar fluxes**: northern and southern polar fluxes are scaled by their cycle maxima to focus on fluctuations within the cycles. The absolute values of the scaled polar fluxes are used.
- **Difference in polar fluxes**: the differences between the absolute unscaled northern and southern polar fluxes are included.

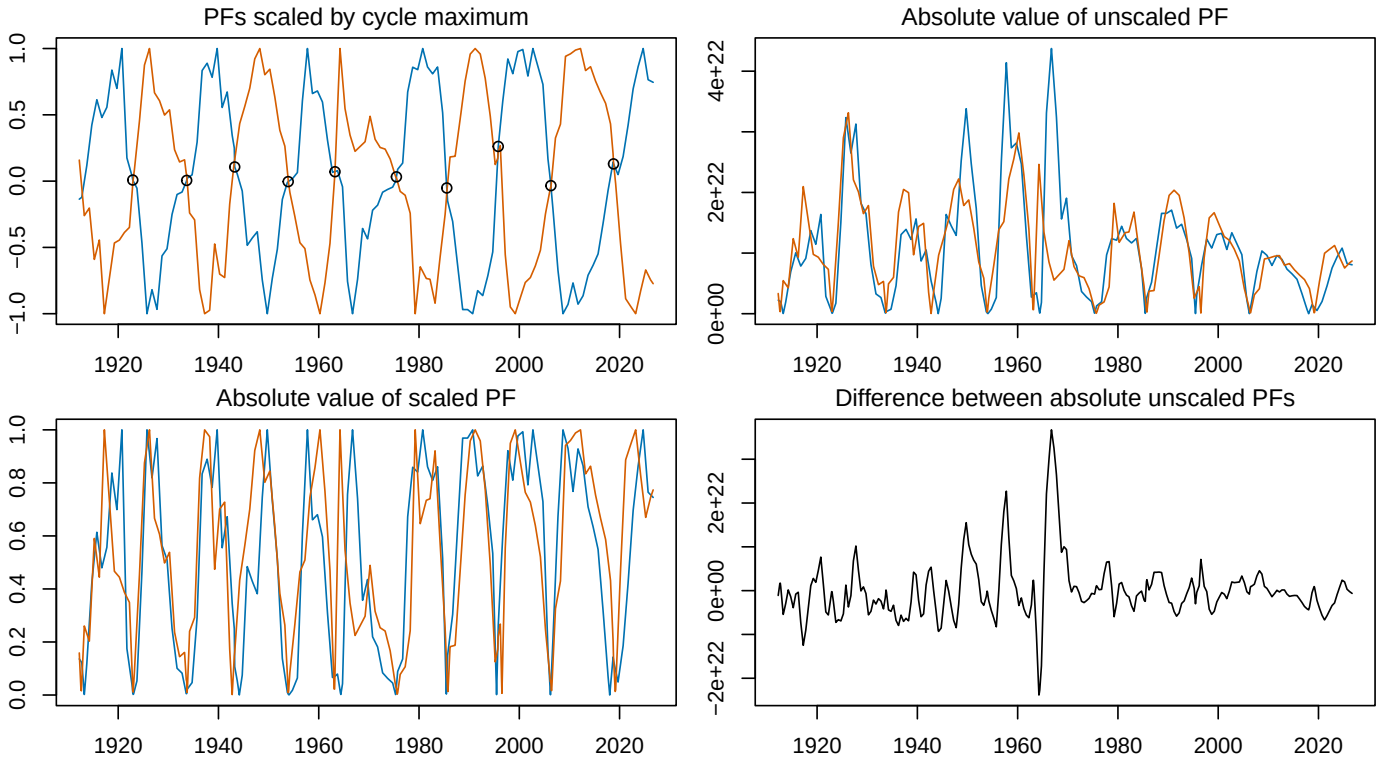

Model Fitting

- We first fit the Yu et al. model using MCMC to generate posterior samples of the expected SSNs and residuals.
- 100 sets of residuals are randomly selected and a GP model is fit to each set of the residuals.
- The GP models are fitted using the No-U-Turn sampler variant of Hamiltonian Monte Carlo. For each GP, 2000 posterior samples of the expected residuals are generated. The residuals are added back to the corresponding SSNs estimates to form new estimates.
- In total, 100×2000 simulations of estimated SSNs are generated. A fitted mean curve is obtained using the pointwise averages. Quantiles of the simulations are used to form the confidence bands.

Results - Predictions

- Improvement in predictive performance is confirmed by the skill score, $\mathrm{SS} = 1 - \frac{\mathrm{MSE(forecast,observed)}}{\mathrm{MSE(reference,observed)}}$. Cycle 23: SS = 0.098; Cycle 24: SS = 0.193.

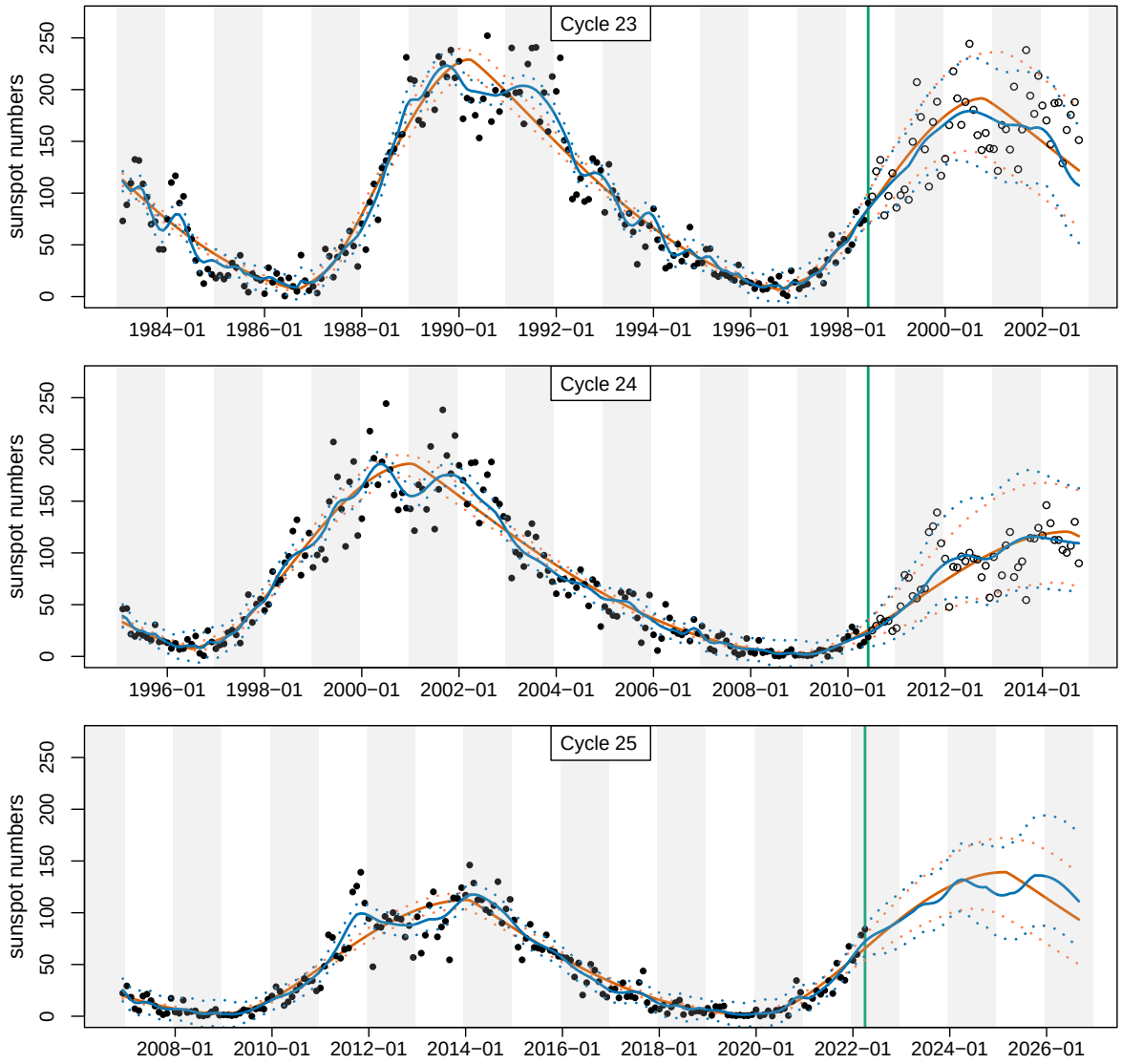

Results - RDVS

- We carry out reference distribution variable selection (RDVS) (Linkletter et al. 2006) to assess the significance of the GP input variables by considering an uncorrelated, inert variable.
- The process is repeated for many times to generate an importance metric for each variable based on the posterior medians of the length-scale parameters.
- The 10th percentile of the importance of the inert variable is used as a cutoff for selecting important variables.

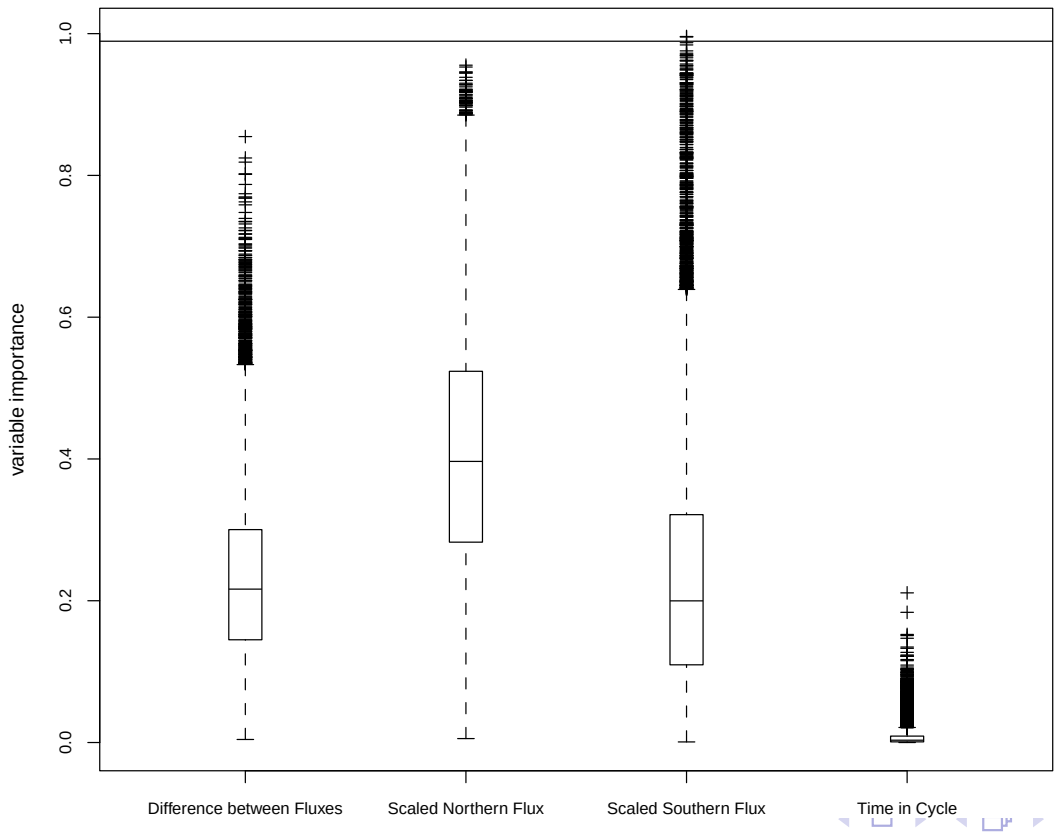

Results - BIC

- We compute BIC for the GP models using posterior samples of the model parameters. This allows us to make a histogram of BIC for each fitted GP.
- We also fit the residuals with a $N(0, \sigma^2)$ model and compute BIC to provide a comparison.

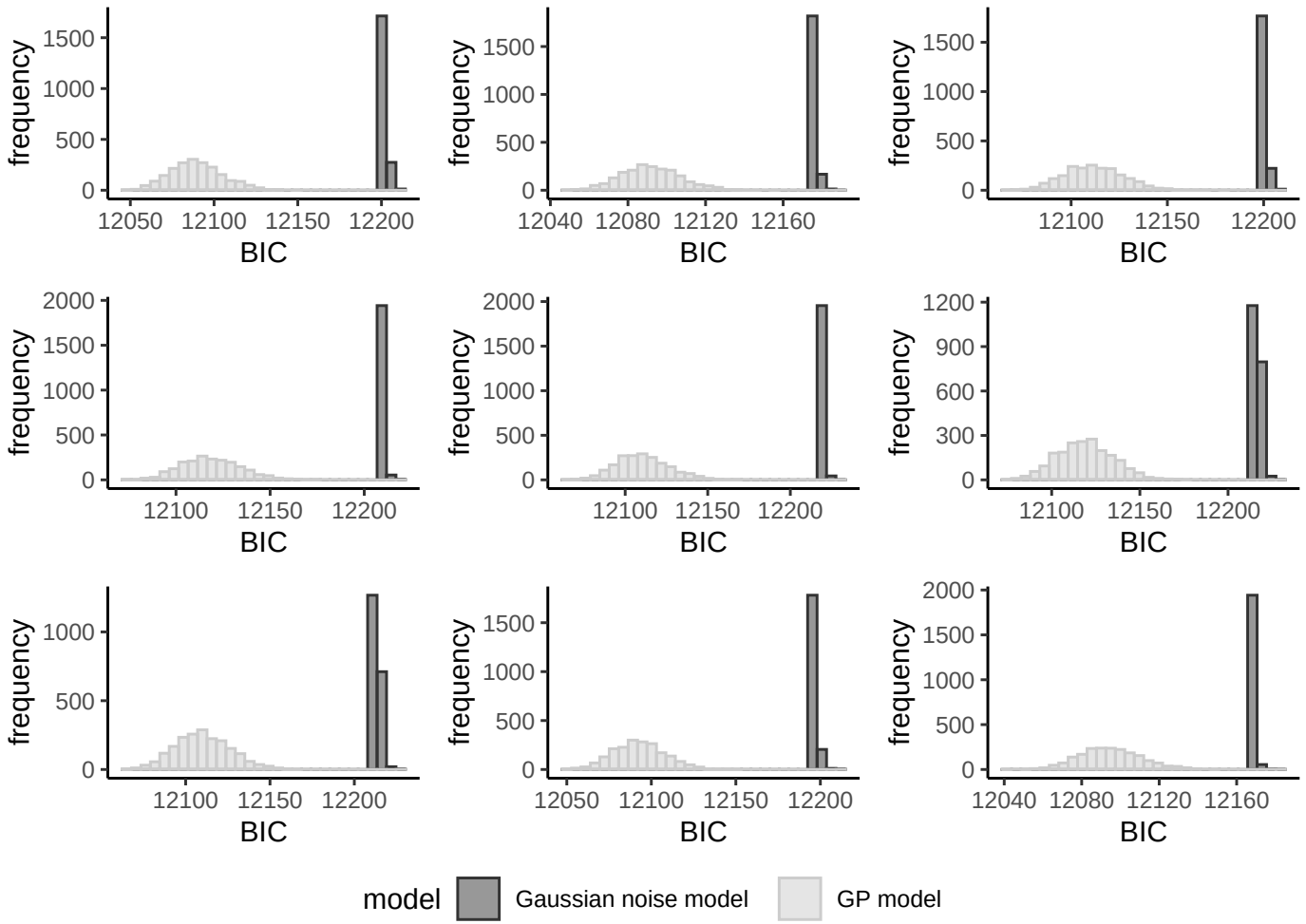

Discussion

- The multiple peaks predicted by the model appear to capture real features of the observed data. The validity of our modeling approach is verified by the quantitative tests we run.
- Limitations of our approach include the fact that using the polar flux data limits the window in which the predictions can be made. In addition, the Yu et al. model and the GP model are fitted separately instead of simultaneously.